

## COSMOLOGICAL VELOCITY-DENSITY RELATION IN THE QUASI-LINEAR REGIME

ADI NUSSER AND AVISHAI DEKEL

Racah Institute of Physics, The Hebrew University of Jerusalem, Jerusalem 91904, Israel

EDMUND BERTSCHINGER

Department of Physics, Massachusetts Institute of Technology, 6-207, Cambridge, MA 02139

AND

GEORGE R. BLUMENTHAL

Lick Observatory/UCO, Board of Studies in Astronomy and Astrophysics, University of California, Santa Cruz, CA 95064

Received 1990 October 17; accepted 1991 March 19

### ABSTRACT

We develop practical methods for extracting the mass-density fluctuation field of a cosmological system,  $\delta(\mathbf{x})$ , from the peculiar velocity field smoothed on scales of a few Mpc. The methods are local. They are based on quasi-linear approximations to the gravitational equations of motion of a pressureless fluid and address density fluctuations in the range  $-0.7 \leq \delta \leq 4.5$ . They are tested against exact solutions in special configurations and against cosmological  $N$ -body simulations with  $\Omega = 1$  and with  $\Omega = 0.2$ . Two approximations are considered under the assumption of Zel'dovich displacements of particles with a universal time dependence: the exact solution of the continuity equation,  $\delta_c$ , and the exact solution of the dynamical Euler-Poisson equation,  $\delta_a$ , which turns out to coincide with the linear approximation,  $\delta_0$ . A key new result is our derivation of the density fluctuation field, based on the Lagrangian Zel'dovich approximation, in terms of the partial derivatives of the Eulerian velocity field. We find that both  $\delta_a$  and  $\delta_c$  are tightly related to the true density, with a standard deviation  $\leq 0.1$ . While  $\delta_a$  systematically underestimates the true density,  $\delta_c$  is an excellent approximation to  $\delta$ , with an rms error  $\lesssim 0.1$ . Alternatively, we find an empirical third-order approximation for  $\delta(\delta_0)$  with a similar rms error. Corrections involving second derivatives are less successful, with an rms error  $\sim 0.3$ . The continuity density scheme is now being used in the POTENT analysis of the large-scale velocities.

The tight relation between the true density and the linear approximation in the quasi-linear regime also suggests a method for the inverse problem of extracting the quasi-linear velocity from a given density field specified over a large region. This new inversion procedure can improve the prediction of the peculiar velocity field from galaxy redshift surveys such as the *IRAS* survey.

*Subject headings:* cosmology — dark matter — galaxies: clustering — galaxies: formation

### 1. INTRODUCTION

One of the most interesting unknowns in cosmology today is the distribution of matter on large scales. The accumulating large galaxy redshift surveys provide information about the large-scale distribution of *luminous* matter, but we have no direct evidence for the distribution of *dark* matter that dominates the mass density in the universe. There is no reason to assume that the density of galaxies is proportional to the underlying mass density; galaxy formation might be biased toward certain regions (see, e.g., the review by Dekel & Rees 1987). The only way to learn about the mass distribution is via its gravitational influence on test bodies whose velocities one can observe. This is how the rotation curves of galaxies are used to trace massive dark halos and how virial velocities are used to indicate dark mass in clusters of galaxies. The recent improvements of the techniques to measure distances to galaxies independently of their measured redshifts (cf. Pierce & Tully 1988; Dressler et al. 1987) allow the compilation of large samples of galaxies with measured peculiar velocities (e.g., Lynden-Bell et al. 1988), which can be used to trace the underlying smoothed velocity field. If the structure on large scales is generated by gravity, then these velocities can, in principle, be used to map the mass density perturbation field that is responsible for inducing them.

Of the three components of the peculiar velocity, only the radial component,  $u$ , is directly observable. One method to

obtain the two missing components is the POTENT analysis (Bertschinger & Dekel 1989; Dekel, Bertschinger, & Faber 1990; Bertschinger et al. 1990). If the peculiar velocities are generated by gravity, and if the velocity field is smoothed sufficiently to remove small-scale orbit-mixing, the velocity is derived from a scalar potential:  $\mathbf{v}(\mathbf{x}) = -\nabla\phi_v(\mathbf{x})$ . The velocity potential  $\phi_v$  may be recovered by integrating the smoothed radial velocity component along radial rays,

$$\phi_v(\mathbf{x}) = -\int_0^r u(r', \vartheta, \varphi) dr', \quad (1)$$

and the transverse velocity components are computed by differentiation along  $\vartheta$  and  $\varphi$ . The outcome is the three-dimensional velocity field on a uniform Eulerian grid inside a given volume. This procedure is kinematical and is based only on the *Ansatz* of potential flow. Within the general framework of gravitational instability, after smoothing over regions of orbit-mixing, no further approximations are involved.

In order to recover the associated mass density field out of the given velocity field, one needs to appeal to gravity more specifically—the dynamics is introduced via the cosmological Euler and Poisson equations. When the fluctuations are small, the linear approximation yields a simple, local relation between the density contrast and the peculiar velocity,  $\delta \propto -\nabla \cdot \mathbf{v}$ . However, the range of interest for phenomena like the Great Attractor or the large voids is slightly beyond the

linear regime, where, even when averaged over scales of order  $10 h^{-1}$  Mpc, the density fluctuations can be of order unity or a few. In this case, higher order contributions can be just as important. Unfortunately, already the second-order solution is not very useful for our purpose because it is not local any more—it involves integrals over a large volume (Peebles 1980).

One hope for a *local, quasi-linear* approximation lies in the Zel'dovich (1970) approach, which follows trajectories of particles from their initial, Lagrangian positions to their present, Eulerian positions. Unlike the linear approximation, the Zel'dovich approximation takes into account particle displacements, and it assumes that the displacements (rather than the density fluctuations) all grow at a universal rate. Trying to solve for the density assuming such approximate displacements (hereafter “Zel'dovich displacements”) one has a choice between different options. For example, if one requires mass conservation by solving the continuity equation, the approximation would, in general, violate momentum conservation. On the other hand, if one assumes momentum conservation by solving the equation of motion, the approximation would, in general, fail to conserve mass. Thus, given the velocity field, what is the best approximation for the density under the assumption of Zel'dovich displacements? Our major aim in this paper is to address this question and to come up with a practical algorithm for calculating the density. We also consider nonlinear corrections involving cubic polynomials or second derivatives, which we eventually test using  $N$ -body simulations.

The inverse procedure of extracting the velocity from a given density field is very useful in complementary dynamical analysis of large, uniform redshift surveys, such as the *IRAS* survey (e.g., Strauss et al. 1990; Yahil et al. 1990). There, the mass density is taken from the observed galaxy density, corrected for sampling, under the assumption that galaxies trace the mass. This inverse procedure is intrinsically more difficult because, even in the linear regime, it involves a nonlocal integral of the density over a volume which can be quite large. Still, one wishes to improve on the linear analysis used so far, and we suggest a practical method for incorporating quasi-linear corrections to this procedure.

The paper is organized as follows. In § 2 we derive the approximations for getting densities from velocities. We then test them in simple toy models (§ 3) and using  $N$ -body simulations (§ 4), and obtain empirical fits based on the simulations. In § 5 we briefly address the inverse problem of extracting the velocity field from the density field, and we summarize our recommended working procedures in § 6.

## 2. QUASI-LINEAR DENSITIES

Given the peculiar velocity field  $\mathbf{v}(\mathbf{x}, t_0)$  (i.e., relative to the local Hubble-expanding frame), in Eulerian coordinates  $\mathbf{x}$  at time  $t_0$ , we wish to calculate the density fluctuation field  $\delta(\mathbf{x}, t_0) \equiv [\rho(\mathbf{x}, t_0) - \bar{\rho}(t_0)]/\bar{\rho}(t_0)$ , where  $\rho$  is the local density and  $\bar{\rho}$  is the mean density in the universe. The range of interest is the quasi-linear regime, where  $\delta$  is of order unity, and perhaps up to values  $\sim 4.5$ —the turnaround value in the top-hat model for  $\Omega = 1$ . The goal is to avoid simulations or iterations and to use local information as much as possible.

### 2.1. The Equations

For the purpose of setting up the background and notations, let us start with the relevant basics of the standard theory of gravitational instability. Let  $\mathbf{x}$ ,  $\mathbf{v}$ , and  $\phi_g$  be the position, pecu-

liar velocity and peculiar gravitational potential in comoving distance units; the corresponding quantities in physical units are  $a\mathbf{x}$ ,  $a\mathbf{v}$ , and  $a^2\phi_g$ , where  $a(t)$  is the universal expansion factor. The three equations governing the evolution of a pressureless gravitating fluid in a standard cosmological background are then the *continuity* equation,

$$\frac{\partial \delta}{\partial t} + \nabla \cdot \mathbf{v} + \nabla \cdot (\delta \mathbf{v}) = 0, \quad (2)$$

the *Euler* equation of motion,

$$\frac{\partial \mathbf{v}}{\partial t} + 2H\mathbf{v} + (\mathbf{v} \cdot \nabla)\mathbf{v} = -\nabla\phi_g, \quad (3)$$

and the *Poisson* field equation,

$$\nabla^2 \phi_g = \frac{3}{2}H^2\Omega\delta, \quad (4)$$

where  $H$  and  $\Omega$  are the Hubble parameter and the cosmological density parameter, both varying in time. [See, e.g., Peebles 1980, § 9, but note that noncomoving velocity and potential are used there instead. With comoving coordinates, we have a factor of 2 in the second term of eq. (3), but  $a(t)$  does not show up explicitly except in  $H$ .]

The pressure term is left out of equation (3), assuming that particle orbits do not cross. Note also that the second order term in equation (3) can be written as,

$$(\mathbf{v} \cdot \nabla)\mathbf{v} = \frac{1}{2}\nabla v^2 - \mathbf{v} \times (\nabla \times \mathbf{v}), \quad (5)$$

so, if the velocity field has no vorticity, this term could be replaced by  $(\frac{1}{2})\nabla v^2$ . By combining the Poisson equation and the divergence of the Euler equation we can eliminate the term containing the gravitational potential and replace equations (3) and (4) by the *dynamical* equation for the case of no pressure and no vorticity,

$$\frac{3}{2}H^2\Omega\delta = -\frac{\partial}{\partial t}(\nabla \cdot \mathbf{v}) - 2H\nabla \cdot \mathbf{v} - \frac{1}{2}\nabla^2 v^2. \quad (6)$$

It is sometimes useful to relate the gravitational and velocity potentials by the *Bernoulli* equation, which is derived here from the Euler equation assuming no pressure and no vorticity,

$$\phi_g = \frac{\partial}{\partial t}\phi_v + 2H\phi_v - \frac{1}{2}v^2, \quad \mathbf{v} \equiv -\nabla\phi_v. \quad (7)$$

### 2.2. The Linear Approximation

In the linear approximation, i.e., neglecting the terms involving  $\delta\mathbf{v}$  and  $v^2$ , equations (2)–(4) yield the standard linear time evolution equation for  $\delta(\mathbf{x}, t)$ ,

$$\dot{\delta} + 2H\delta = \frac{3}{2}H^2\Omega\delta. \quad (8)$$

The growing mode of the solution to this equation is denoted  $\delta \propto D(t)$ . It can be expressed in terms of the function  $f(\Omega)$ ,

$$f(\Omega) \equiv \frac{\dot{D}}{HD}, \quad (9)$$

which is commonly approximated by  $f(\Omega) \simeq \Omega^{0.6}$  (Peebles 1980). [Lightman & Schechter (1990) have shown recently that near  $\Omega = 1$  the linear term is actually  $f(\Omega) = \Omega^{4/7}$ .] The dynamical equation can be written as

$$\frac{\ddot{D}}{D} = H^2 \left[ -2f(\Omega) + \frac{3}{2}\Omega \right], \quad (10)$$

and the continuity equation yields the well-known linear relation between density and velocity:

$$\delta = \delta_0 \equiv -(Hf)^{-1} \nabla \cdot \mathbf{v}. \quad (11)$$

The density is determined by the local current of matter.

### 2.3. The Zel'dovich Approximation

A quasi-linear approximation that is still local is provided by the Zel'dovich approximation (Zel'dovich 1970), which, unlike the pure linear approximation, takes into account the displacements of particles from their initial positions. Let  $\mathbf{q}$  be the initial (i.e. Lagrangian), comoving position of a particle. The Zel'dovich approximation assumes that the comoving position of that particle at time  $t$  (i.e., the Eulerian position) is

$$\mathbf{x}(\mathbf{q}, t) = \mathbf{q} + D(t)\psi(\mathbf{q}). \quad (12)$$

The approximation is in writing the displacement,  $\mathbf{x}(\mathbf{q}, t) - \mathbf{q}$ , as a product of a spatial perturbation function,  $\psi(\mathbf{q})$ , and a universal time-dependent function,  $D(t)$ . By taking time derivatives following the trajectory of each particle, the comoving peculiar velocity and acceleration are

$$\mathbf{v}(\mathbf{q}, t) = \dot{D}\psi, \quad \mathbf{g}(\mathbf{q}, t) \equiv \frac{d}{dt} \mathbf{v} = \ddot{D}\psi \propto \mathbf{v}. \quad (13)$$

Note that, as in the linear approximation, the velocity vector is proportional to the acceleration vector, so the Zel'dovich motions, in comoving coordinates, are along predetermined straight lines.

The Zel'dovich approximation provides an exact solution to the linearized equations where  $\delta$  and  $\mathbf{v}$  are very small, with  $D(t)$  being the growth rate of the linear solution of  $\delta(t)$ . Therefore, the universal growth of the displacements must be given by the linear  $D(t)$  of equation (9) under quasi-linear conditions as well. However, the particles move away from their initial positions, so the density at a given position does not necessarily evolve according to the linear growth rate. In fact, infinite density can develop in a finite time as a result of a convergence of particle trajectories into singular points.

In general, the Zel'dovich approximation is *not* an exact solution of the set of equations (2)–(4). In particular, by substituting the Zel'dovich expressions for  $\mathbf{v}(\mathbf{x})$  and  $\mathbf{g}(\mathbf{x})$  from equations (12) and (13) alternatively in the continuity equation and in the dynamical equation (6), one obtains two different approximations for the density field; the former conserves mass and the latter conserves momentum.

### 2.4. Continuity Density in the Zel'dovich Approximation

In the following, we shall assume that there is a one-to-one correspondence between  $\mathbf{x}$  and  $\mathbf{q}$ , i.e., *no orbit-mixing*. To achieve this in practice, and to avoid very large values of  $\delta$ , we will be dealing with the velocity field that has been smoothed over a large enough scale. The assumed one-to-one correspondence allows us to write the Zel'dovich approximation (12) in Eulerian space,

$$\mathbf{q}(\mathbf{x}) = \mathbf{x} - D\psi[\mathbf{q}(\mathbf{x})]. \quad (14)$$

Note that this is an unusual way to write the Zel'dovich displacements, because the Zel'dovich approximation is commonly understood as a Lagrangian scheme in which one follows the trajectories of individual particles. But this way of expressing the approximation is exactly what we need if we want to obtain the density from a given Eulerian velocity field.

The continuity equation, in the Zel'dovich language, can be written as

$$\rho_x(\mathbf{x})d^3x = \rho_q d^3q, \quad (15)$$

where  $\rho_x$  is the Eulerian density and  $\rho_q$  is the Lagrangian density (i.e., the universal mean density). The density contrast is therefore

$$\begin{aligned} \delta_c(\mathbf{x}) &= \left\| \frac{\partial \mathbf{q}}{\partial \mathbf{x}} \right\| - 1 \\ &= \left\| I - D \frac{\partial \psi}{\partial \mathbf{x}} \right\| - 1 \\ &= \left\| I - (Hf)^{-1} \frac{\partial \mathbf{v}}{\partial \mathbf{x}} \right\| - 1, \end{aligned} \quad (16)$$

where the double vertical bars denote the Jacobian determinant and  $I$  is the unit matrix. Note that this is a nonlinear expression which still involves only the first partial derivatives.

If we assume that the velocity field is a *potential flow*, with no vorticity, then the deformation tensor  $\partial\psi/\partial\mathbf{x}$  is symmetric (just like  $\partial\psi/\partial\mathbf{q}$ ), and it can therefore be diagonalized locally. Denote the eigenvalues of the Eulerian deformation tensor  $\mu_i(\mathbf{x})$ , where  $i = 1, 2, 3$  correspond to the eigenvectors. The continuity density is then

$$\delta_c = (1 - D\mu_1)(1 - D\mu_2)(1 - D\mu_3) - 1. \quad (17)$$

This can be written as a third-order power series in  $D$ ,

$$\delta_c = -DM_1 + D^2M_2 - D^3M_3, \quad (18a)$$

$$\begin{aligned} M_1 &\equiv \mu_1 + \mu_2 + \mu_3, & M_2 &\equiv \mu_1\mu_2 + \mu_1\mu_3 + \mu_2\mu_3, \\ M_3 &\equiv \mu_1\mu_2\mu_3. \end{aligned} \quad (18b)$$

### 2.5. Dynamical Density in the Zel'dovich Approximation

If we substitute the Zel'dovich approximation (14) into the dynamical equation (6) instead, we find, after some algebra, that the second-order terms involving second derivatives exactly cancel each other, leaving

$$\delta_d(\mathbf{x}) = -(Hf)^{-1} \nabla \cdot \mathbf{v} = -DM_1, \quad (19)$$

exactly as in the linear approximation, i.e.,  $\delta_d = \delta_0$ . (This is independent of the assumption of no-vorticity.) Thus, the linear relation between velocity and density is of interest in the quasi-linear regime as well; it relates the velocity field associated with Zel'dovich displacements with the density fluctuation field that would have generated such velocities via real gravity. The fact that  $\delta_d = \delta_0$  becomes trivial by noting that the two terms  $\dot{\mathbf{v}} + (\mathbf{v} \cdot \nabla)\mathbf{v}$  in equation (3) represent the acceleration of a particle (that particle that is at position  $\mathbf{x}$  at time  $t$ ), which, by equation (13) of the Zel'dovich approximation, is proportional to its velocity. Therefore, by substituting the divergence of equation (3) into equation (4), we must get  $\delta_d \propto -\nabla \cdot \mathbf{v}$ .

The difference between the two approximations, the continuity density and the dynamical density,

$$\delta_c - \delta_d = D^2M_2 - D^3M_3, \quad (20)$$

can be interpreted as an estimate for the "error" associated with the Zel'dovich approximation (cf. Shandarin, Doroshkevich, & Zel'dovich 1983). It is of order  $O(D^2)$ , and indeed it vanishes when  $D \ll 1$ .

### 2.6. Second-Order Corrections

The full second-order solution to the equations (2)–(4) for  $\Omega = 1$  is (see Peebles 1980, eq. [18.8])

$$\delta = \delta_0 + \frac{5}{7} \delta_0^2 + \frac{2}{3H^2} (\partial_i \delta_0)(\partial_i \phi_g) + \frac{8}{63H^4} (\partial_{ij} \phi_g)(\partial_{ij} \phi_g), \quad (21a)$$

where

$$\phi_g(\mathbf{x}) = -\frac{3H^2\Omega}{8\pi} \int \frac{d^3x' \delta(\mathbf{x}')}{|\mathbf{x} - \mathbf{x}'|}, \quad (21b)$$

and the summation rule applies for  $i, j = 1, 2, 3$ . This, unfortunately, is less useful than the linear approximation or the Zel'dovich scheme because of the nonlocal terms involved; they require calculating the gravitational force by integration over a large volume, which suffers from boundary effects.

Since the application of the full second-order solution is impractical, one might be tempted to try various second-order corrections to the linear solution, hoping for partial improvement in the approximation. Note that the only unknown quantity in the dynamical equation is the time derivative;  $\dot{v}$  in equation (6), or equivalently,  $\dot{\phi}_v$  in the Bernoulli equation. One might hope that by substituting a known lower-order approximation for the time derivative in equation (6), keeping the explicit term  $-(\frac{1}{2})\nabla^2 v^2$ , the approximation might improve. This correction involves second derivatives of  $v$ , while the Zel'dovich approximation includes only powers of the first derivatives.

Unfortunately, this procedure is not unique. Take, for example, the linear time derivative expressed in terms of  $\nabla \cdot \mathbf{v}$  (or  $\delta_0$ ), i.e.,  $\partial(\nabla \cdot \mathbf{v})/\partial t = (-2 + 3\Omega/2f)H\nabla \cdot \mathbf{v}$ . Then the solution of equation (6) is

$$\delta = \delta_0 - \frac{1}{3H^2\Omega} \nabla^2 v^2. \quad (22)$$

The same result is obtained if we use the linear relation  $\dot{\phi}_v = (3\Omega H/2f)\phi_v$  in the Bernoulli equation. But take, instead, the linear time derivative expressed in terms of  $\delta$ , i.e.  $\partial(\nabla \cdot \mathbf{v})\partial t = (2f - 3\Omega/2)H^2\delta$ . Then, in equation (6),

$$\delta = \delta_0 - \frac{1}{4H^2f} \nabla^2 v^2. \quad (23)$$

The correction terms in the two cases differ both in the numerical factor and in the  $\Omega$  dependence. Hence, the result is quite arbitrary, for an obvious reason; the linear approximation for the time derivative neglects terms  $\propto \nabla^2 v^2$ , so one should not expect to obtain a meaningful correction of that order even if the explicit term of this sort in equation (6) is not neglected.

Recall that if we use the Zel'dovich approximation for the time derivative in equation (6), as in § 2.5, the  $\nabla^2 v^2$  terms cancel each other and we get back the dynamical density  $\delta = \delta_d = \delta_0$  with no quadratic correction. This is probably a better second-order approximation than equations (22) or (23).

In fact, the corrections obtained using linear time dependence might be in the wrong direction altogether. Consider, for example, a top-hat model, in which the density is uniform and the velocity is a radial ‘‘Hubble’’ flow,  $v \propto -r$ . In this case  $\nabla^2 v^2$  is positive, so the ‘‘correction’’ terms in equations (22) and (23) are negative—actually pushing the approximation away from the true nonlinear solution. We shall see below that this is the typical behavior in the  $N$ -body simulations and will

try to use the simulations to obtain empirically the best-fit (positive) coefficient to a general correction term of the sort  $\propto \nabla^2 v^2$ .

## 3. TESTING IN SYMMETRIC TOY MODELS

### 3.1. Prototypical Configurations

It is instructive to investigate the errors of the approximate densities under the Zel'dovich approximation in various generic cases of special symmetries, which can be classified by the relations between the eigenvalues of the deformation tensor.

Consider a one-dimensional collapse or expansion, where one eigenvalue dominates,  $|\mu_1| \gg |\mu_2| \simeq |\mu_3|$ . This can form a *pancake* or an *antipancake* (i.e., a cylindrical void expanding along its height). In this case,

$$\delta_c \simeq \delta_d \simeq -D\mu_1 \simeq \delta_0. \quad (24)$$

Thus, in the pure one-dimensional case ( $\mu_2 = \mu_3 = 0$ ), the Zel'dovich scheme is exact (cf. Zel'dovich 1970). The two density estimators coincide, and they are both an exact solution of the equations.

Consider, next, two-dimensional cases, where  $|\mu_1| \simeq |\mu_2| \gg |\mu_3|$ . When  $\mu_1$  and  $\mu_2$  have the same sign, the configuration is a *filament* or an *antifilament* (i.e., a cylindrical void expanding parallel to its base), and then

$$\begin{aligned} \delta_d &\simeq -2D\mu_1 \simeq \delta_0 \\ \delta_c &\simeq -2D\mu_1 + D^2\mu_1^2 \simeq \delta_0 + \frac{1}{4}\delta_0^2. \end{aligned} \quad (25)$$

The relative ‘‘error’’ estimate is  $\Delta \equiv (\delta_c - \delta_d)/\delta_d \simeq \delta_0/4$ , i.e., 25% at  $\delta_0 = \pm 1$ . When  $\mu_1$  and  $\mu_2$  have opposite signs, the configuration is a combination of a pancake and an antipancake, and

$$\begin{aligned} \delta_d &\simeq 0 \simeq \delta_0 \\ \delta_c &\simeq -D^2\mu_1^2. \end{aligned} \quad (26)$$

Here  $\delta_c$  is not a simple function of  $\delta_0$ .

Finally, consider the case of three eigenvalues of similar amplitudes,  $|\mu_1| \simeq |\mu_2| \simeq |\mu_3|$ . When the three eigenvalues all have the same sign, we get a *spherical cluster* or a *spherical void*, with

$$\begin{aligned} \delta_d &\simeq -3D\mu_1 \simeq \delta_0 \\ \delta_c &\simeq -3D\mu_1 + 3D^2\mu_1^2 - D^3\mu_1^3 \simeq \delta_0 + \frac{1}{3}\delta_0^2 + \frac{1}{27}\delta_0^3. \end{aligned} \quad (27)$$

The relative error is  $\Delta = \delta_0/3 + \delta_0^2/27$ , i.e., 37% at  $\delta_0 = 1$  for a collapsing cluster, and a maximum of 30% at  $\delta_0 = -1$  for an expanding void.

When one eigenvalue is of an opposite sign,  $\mu_1 \simeq \mu_2 \simeq -\mu_3$ , we have an *expanding pancake* or an *expanding filament*, with

$$\begin{aligned} \delta_d &\simeq -D\mu_1 \simeq \delta_0, \\ \delta_c &\simeq -D\mu_1 - D^2\mu_1^2 + D^3\mu_1^3 \simeq \delta_0 - \delta_0^2 - \delta_0^3. \end{aligned} \quad (28)$$

In this case  $\Delta \simeq -(\delta_0 + \delta_0^2)$ . The case of an expanding filament ( $\delta_0 > 0$ ) carries the worst relative error: 100% at  $\delta_0 = 0.62$  and 200% already at  $\delta_0 = 1$ . The maximum relative error for an expanding pancake ( $\delta_0 < 0$ ) is 25%, at  $\delta_0 = -0.5$ .

### 3.2. Top-Hat Model

In the spherically symmetric case, we have an exact solution to compare to. Assume  $\Omega = 1$  and  $H = 1$ . In a top-hat model of uniform density embedded in an Einstein–de Sitter universe,

one can find a parametric solution for the density contrast at time  $t$ ,  $\delta_{\text{th}}(t)$ . First express the cosmological time in terms of the local arc parameter  $\eta$ . For positive and negative density perturbations respectively, denoted  $k = \pm 1$ ,

$$t = ka^*[\eta - S_k(\eta)] , \quad (29)$$

where  $a^*$  characterizes the amplitude of the given perturbation at a given time, and  $S_k$  stands for  $\sin$  for  $k = +1$  and  $\sinh$  for  $k = -1$ . The top-hat density contrast at time  $t$  is

$$\delta_{\text{th}}(\eta) = \frac{9k[\eta - S_k(\eta)]^2}{2[1 - C_k(\eta)]^3} - 1 , \quad (30)$$

where we use  $C_k$  for  $\cos$  or  $\cosh$ . At early times, both for positive and negative perturbations,  $t \simeq (a^*/6)\eta^3$  and  $|\delta_{\text{th}}| = (3/20)\eta^2$ . Therefore, for comparisons of equivalent positive and negative perturbations in a cosmological context, where  $\langle \delta \rangle = 0$  at any given  $t$ , we would rather choose the same  $a^*$  for  $k = \pm 1$ .

Next, calculate  $\delta_a$  and  $\delta_c$  of the Zel'dovich approximation in this case, as functions of  $\eta$ . The peculiar velocity in the top-hat model is

$$\mathbf{v}_{\text{th}}(\eta, r) = \left\{ \frac{3kS_k(\eta)[\eta - S_k(\eta)]}{2[1 - C_k(\eta)]^2} - 1 \right\} \mathbf{r} . \quad (31)$$

So, its divergence gives

$$\delta_a(\eta) = \delta_0 \equiv -\nabla \cdot \mathbf{v}_{\text{th}} = 3 - \frac{9kS_k(\eta)[\eta - S_k(\eta)]}{2[1 - C_k(\eta)]^2} , \quad (32)$$

On the other hand, using the continuity equation, we get after some algebra

$$\delta_c = \delta_0 + \frac{1}{3}\delta_0^2 + \frac{1}{27}\delta_0^3 , \quad (33)$$

with  $\delta_0$  defined by equation (32). This, not surprisingly, coincides with the result (27) for the spherical case in the Zel'dovich approximation, with  $\mu_1 = \mu_2 = \mu_3$ .

Figure 1 compares  $\delta_c$  and  $\delta_a$  for the spherical case with the exact  $\delta_{\text{th}}$ . The densities in the Zel'dovich approximation always bracket the true density,  $\delta_a < \delta_{\text{th}} < \delta_c$ . At  $\delta_{\text{th}} = -0.8, -0.5, 1.0, 4.5$  we obtain, respectively,  $\delta_a - \delta_{\text{th}} = -0.2, -0.7, -0.14, -1.5$  and  $\delta_c - \delta_{\text{th}} = +0.09, +0.05, +0.14, +2.4$ . Thus, the two Zel'dovich approximations seem to carry errors of similar magnitudes and opposite signs. A practical good approx-

imation to the exact top-hat solution is given by the arithmetic average

$$\delta_m \equiv 0.5(\delta_c + \delta_a) . \quad (34)$$

It deviates by less than 10% from the top-hat solution over the whole range  $-0.9 < \delta_{\text{th}} < 4.5$ .

The top-hat model can be used to follow the evolution of any spherical perturbation of an overdensity profile  $\delta(r)$  as long as shells do not cross. This is the case outside a collapsed core, provided that the mean density contrast inside a sphere of radius  $r$ ,  $\bar{\delta}(r)$ , is a decreasing function of  $r$ . A shell at radius  $r$  evolves like a top hat of density contrast  $\delta_{\text{th}}(\eta) = \bar{\delta}(r)$ . At a given time, equation (30) defines the corresponding  $\eta(r)$ . The radial velocity of that shell,  $v[\eta(r)]$ , is then given by equation (31), and  $\delta_a(r)$  is given by its divergence, taking into account the  $r$  dependence of  $\eta$ .

One can show that  $\delta_a(r)$  relates to  $\delta(r)$  in exactly the same way as the uniform top hat  $\delta_a(\eta)$  relates to  $\delta_{\text{th}}(\eta)$  {i.e.,  $\bar{\delta}[\eta(r)]$ }, even though  $\delta(r) = \bar{\delta}[\eta(r)]$  and  $\delta_a(r) = \delta_a[\eta(r)]$  for some  $r' < r$ . One can also show that  $\delta_c(r)$  is typically similar to the uniform top-hat value of  $\delta_c[\eta(r)]$ . Thus, Figure 1 can be regarded as describing the relations between the densities in a general spherical perturbation, where the abscissa is  $\delta(r)$ ,  $\delta_a$  is exact, and  $\delta_c$  is an approximation. So  $\delta_m$  is a good approximation in the general spherical case.

We have also calculated, semi-analytically, the densities of the Zel'dovich approximation in a cylindrical uniform collapse model. For a given true value of  $\delta$ , the cylindrical  $\delta_c$  and  $\delta_a$  are systematically better approximations to  $\delta$  by about 10% relative to the spherical case; so the cylindrical  $\delta_m$  is still a very good approximation.

Since  $\delta_m$  is an exact solution in a pancake-like configuration and a good approximation in the spherical and the uniform cylindrical cases, one might hope that it would be a good approximation in the general case as well. This is to be tested below using  $N$ -body simulations.

#### 4. TESTING WITH $N$ -BODY SIMULATIONS

##### 4.1. Testing the Densities in the Zel'dovich Approximation

In order to evaluate the approximations for the density within the Zel'dovich approximation under more general conditions, we now test them using cosmological  $N$ -body simula-

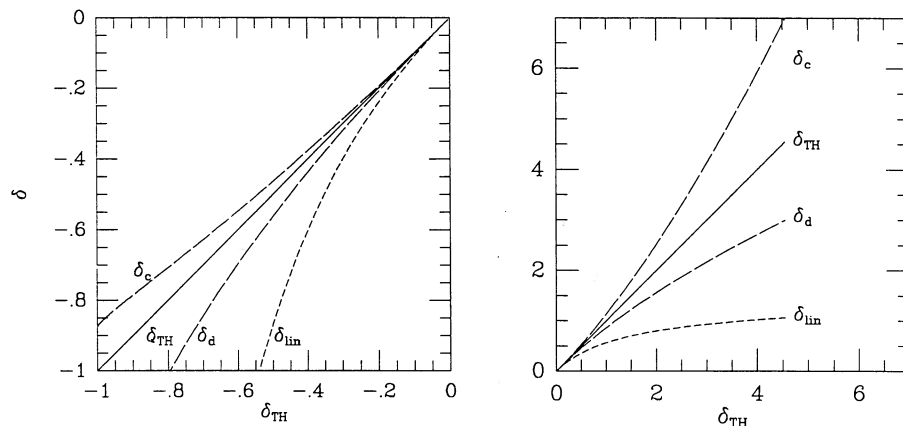


FIG. 1.—Densities as calculated from the velocities under the Zel'dovich approximation in comparison with the exact solution in a top-hat model. The line marked “linear” denotes the density due to the linear growth rate at the time when the top-hat density is what it is; this line does not correspond to the appropriate top-hat velocity.

tions. We use a particle-mesh code (written by E. B.), with  $64^3$  grid cells and  $64^3$  particles in a cubic, comoving box with periodic boundary conditions. At each time step the distribution of particles is translated to density at the grid points using cloud-in-cell interpolation (CIC) and the force at the grid points is then calculated directly from the Fourier transform of the density using fast Fourier transforms (FFTs). The force is interpolated to the particle positions using CIC, and the particles are moved using the standard leapfrog algorithm. The output at the final time is given as positions and velocities of the particles. Using CIC we calculate the density and velocity fields on the points of the cubic grid. The resultant velocity field is a mass-weighted average over the grid-cell scale. We then smooth the density and velocity fields further on a larger scale, using a spherical Gaussian window, to smooth over local inaccuracies of the  $N$ -body code below the Nyquist wavelength and to avoid orbit-mixing and too severe nonlinearities. This smoothing represents volume-weighted averaging. For the purpose of testing the Zel'dovich approximations we consider these smoothed fields to be exact solutions of the equations, but we will return to discuss the limitations of this assumption.

We simulated two alternative cosmological models of initial Gaussian density fluctuations: standard cold dark matter (CDM, spectrum as in Davis et al. 1985) and standard hot dark matter (neutrinos, spectrum from Bond & Szalay 1983), assuming first  $\Omega = 1$ ,  $h = 0.5$ , and normalizing such that  $\delta M/M = 1$  at  $8 h^{-1}$  Mpc based on the linear power spectrum. These two models span the range of plausible fluctuation power spectra within the framework of Gaussian fluctuations (but non-Gaussian initial conditions are not tested here). The comoving box size is  $160 h^{-1}$  Mpc, so the simulation grid spacing is  $250 \text{ km s}^{-1}$ —on the order of the comoving scale of a big galaxy.

Figure 2 shows the particle distribution and the unsmoothed velocity field in one slice of the simulated box, in the two simulations. Figure 3 shows the smoothed density contours and the smoothed velocity vector field in the same slice out of the CDM simulation ( $\delta_{\text{nb}}$ ), and the corresponding Zel'dovich approximations  $\delta_d$  and  $\delta_c$  deduced from the smoothed  $N$ -body velocity field. The velocities, and the actual densities, were smoothed with a Gaussian window of radius 1000 or 500  $\text{km s}^{-1}$ —scales similar to or larger than the galaxy correlation

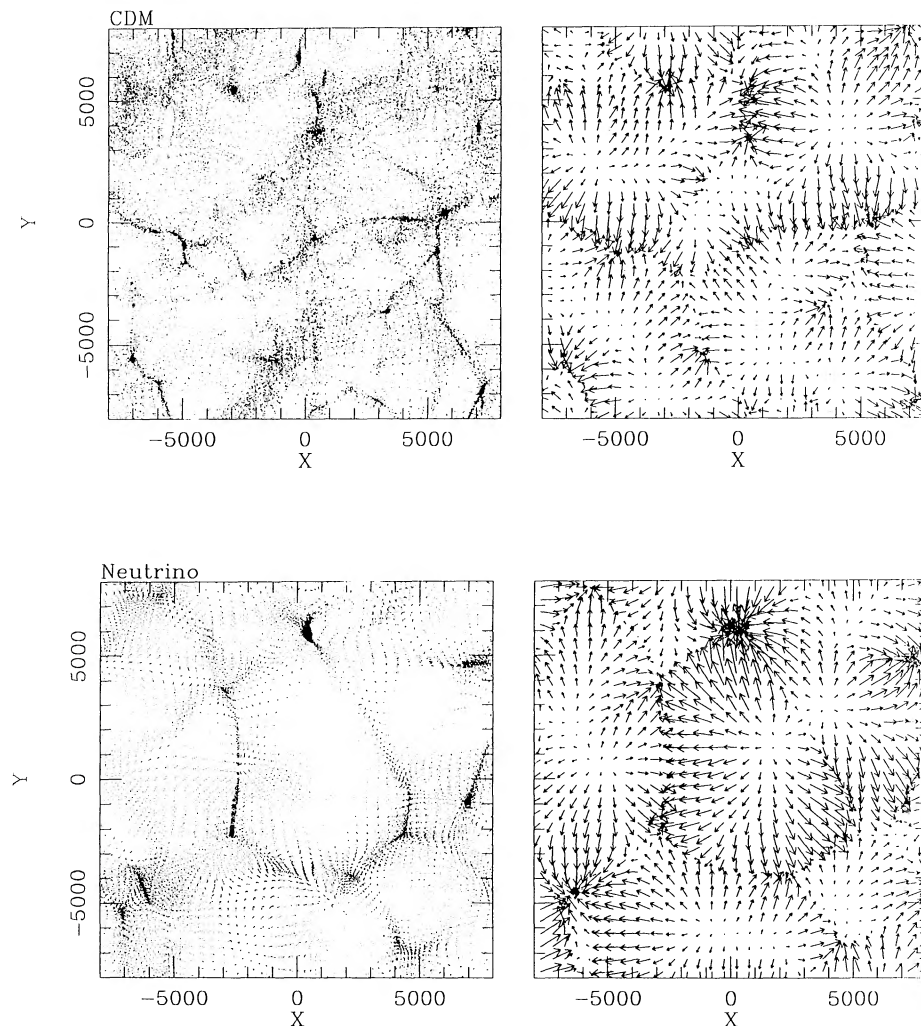


FIG. 2.—Slices of the  $64^3$  cosmological  $N$ -body simulations before smoothing. Length scales are measured in  $\text{km s}^{-1}$ . Slice thickness is  $1250 \text{ km s}^{-1}$ . The time is chosen such that  $\delta M/M = 1$  on a scale of  $800 \text{ km s}^{-1}$  as predicted by linear theory. *Top*: standard CDM. *Bottom*: standard HDM. *Left*: particle distribution. *Right*: peculiar velocity field.

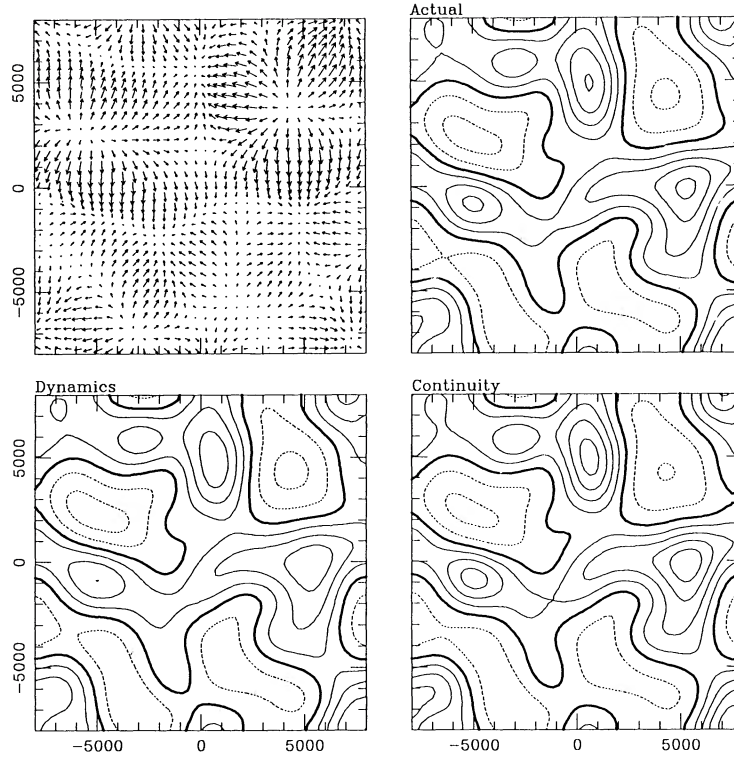


FIG. 3a

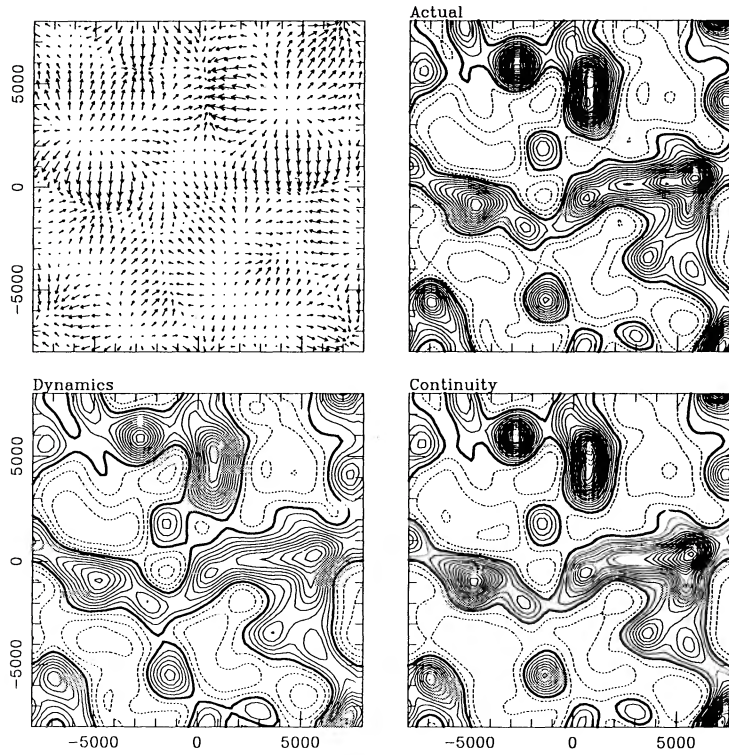


FIG. 3b

FIG. 3.—Peculiar velocity and density-contrast fields in a slice from the CDM  $N$ -body simulation smoothed with a Gaussian of radius  $1000 \text{ km s}^{-1}$  (a) and  $500 \text{ km s}^{-1}$  (b). *Top right*: the true density. *Bottom left*: dynamical density in the Zel'dovich approximation. *Bottom right*: continuity density in the Zel'dovich approximation. Contour spacing is 0.2. The thick line marks  $\delta = 0$ , solid lines mark overdensities, and dashed lines mark underdensities.

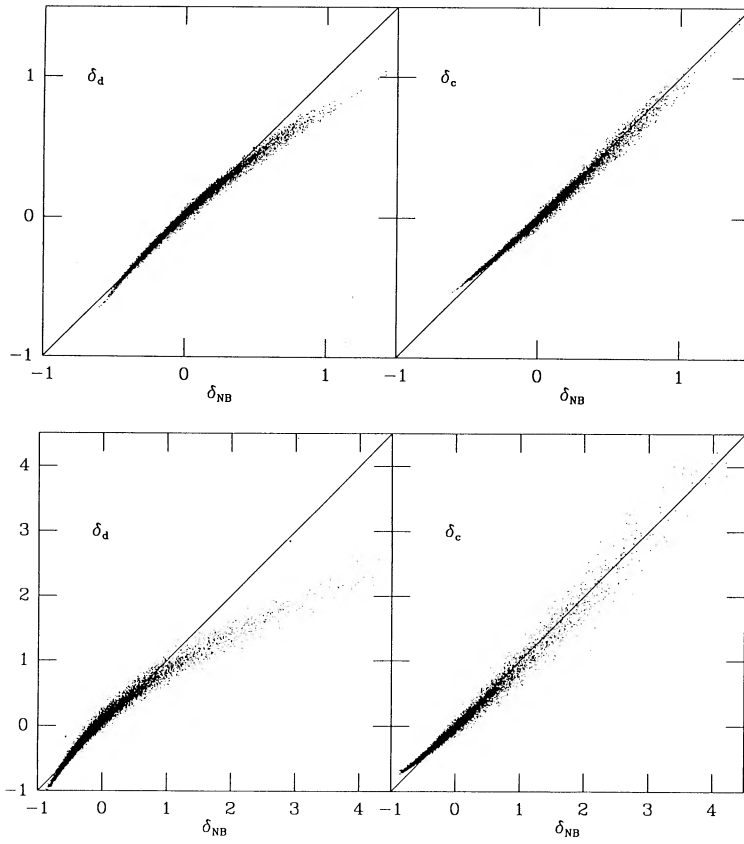


FIG. 4a

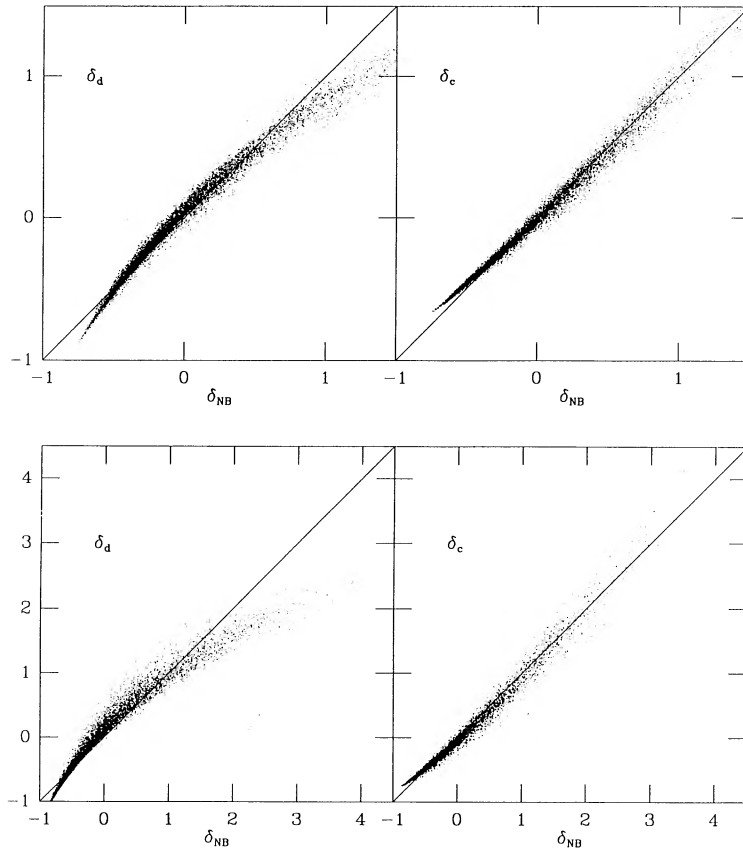


FIG. 4b

FIG. 4.—Densities in the Zel'dovich approximation vs. true densities in the  $N$ -body simulations. CDM (a) and neutrino (b) cosmologies.  $1000 \text{ km s}^{-1}$  (top) and  $500 \text{ km s}^{-1}$  (bottom) Gaussian smoothing.

length that typically corresponds to a few galaxies in the field or to groups or clusters. The partial derivatives of the velocity field, used in computing  $\delta_c$  and  $\delta_d$ , are calculated using cubic splines on the grid of  $250 \text{ km s}^{-1}$  spacing.

In general, both  $\delta_d$  and  $\delta_c$  approximate reasonably well the actual density field for  $|\delta| < 1$ , but  $\delta_c$  is a better approximation for  $\delta > 1$  and  $\delta_d$  is slightly better for  $\delta < -0.3$ .

In the key Figure 4 we plot  $\delta_d$  and  $\delta_c$  versus  $\delta_{\text{nb}}$  for  $10^4$  random grid points of the simulations. The impression from the visual inspection of the contour plots of Figure 3 is now confirmed and quantified. The agreement for  $|\delta| \ll 1$  is very good in both cases, with a slight tendency for  $\delta_c \leq \delta_{\text{nb}} < \delta_d$ . For CDM with 1000 and 500  $\text{km s}^{-1}$  smoothing, respectively, the rms deviations are  $\approx 0.02$  and 0.05. At the high positive peaks,  $\delta_d$  underestimates the density but  $\delta_c$  approximates the density *remarkably well* at least up to  $\delta = 4.5$ . The rms errors are  $\approx 0.05$  and 0.1 for the two smoothing lengths. In deep underdense regions, the typical situation is  $\delta_d \leq \delta_{\text{nb}} < \delta_c$ , with  $\delta_d$  being a somewhat better approximation to  $\delta_{\text{nb}}$ . For CDM with 1000  $\text{km s}^{-1}$  smoothing, at  $\delta = -0.5$  the typical errors are  $\approx 0.06$  and  $-0.03$  for  $\delta_c$  and  $\delta_d$ , respectively.

Two questions come to mind when one tries to interpret the  $N$ -body results in comparison with the exact solutions in the limiting cases discussed earlier. First, what is the reason for the small deviations of  $\delta_d$  from  $\delta_{\text{nb}}$  at  $|\delta| \ll 1$ ? In the linear epoch, when the perturbations are small everywhere,  $\delta_d$  and  $\delta_c$  should both approach the exact solution. Figure 5a, which is similar to

Figure 4, with the same CIC and Gaussian smoothing but at the initial stage of the simulation, confirms that. But why do  $\delta_d$  and  $\delta_c$  not exactly vanish at all points where  $\delta_{\text{nb}} = 0$ ? One reason might be the intrinsic inaccuracies in the  $N$ -body method on scales comparable to the grid-cell size, and, probably more important, the additional CIC smoothing of the velocity field onto the grid at the end of the simulation. Figure 5b shows  $\delta_c$  versus  $\delta_{\text{nb}}$  at the initial time, after the CIC smoothing but before the Gaussian smoothing. The initial displacements are performed by the Zel'dovich approximation itself, so  $\delta_c$  should be an exact solution. The scatter in Figure 5b must therefore be a measure of the CIC inaccuracies, which are apparently nonnegligible. (Note that this is not a problem in the simulated time evolution itself. The CIC errors are expected to be especially large at the beginning of the simulation because the particles are barely displaced from a uniform grid. Although these errors show up strongly in Fig. 5b, they have little effect in the simulation itself because an optimal Green's function is used to correct the gravitational potential and because the initial velocity field is computed using FFTs with no CIC interpolation.)

Another point related to the same issue is whether  $\delta \propto -\nabla \cdot \mathbf{v}$  is indeed a solution at a point where  $|\delta| \ll 1$  but at a nonlinear epoch, when the density is nonlinear at other points. In particular, is  $\delta \propto -\nabla \cdot \mathbf{v}$  valid at a point where today  $\delta = 0$ , but where, most likely,  $\delta$  was nonzero at some other time? The key point is that linear theory is inapplicable if there are non-

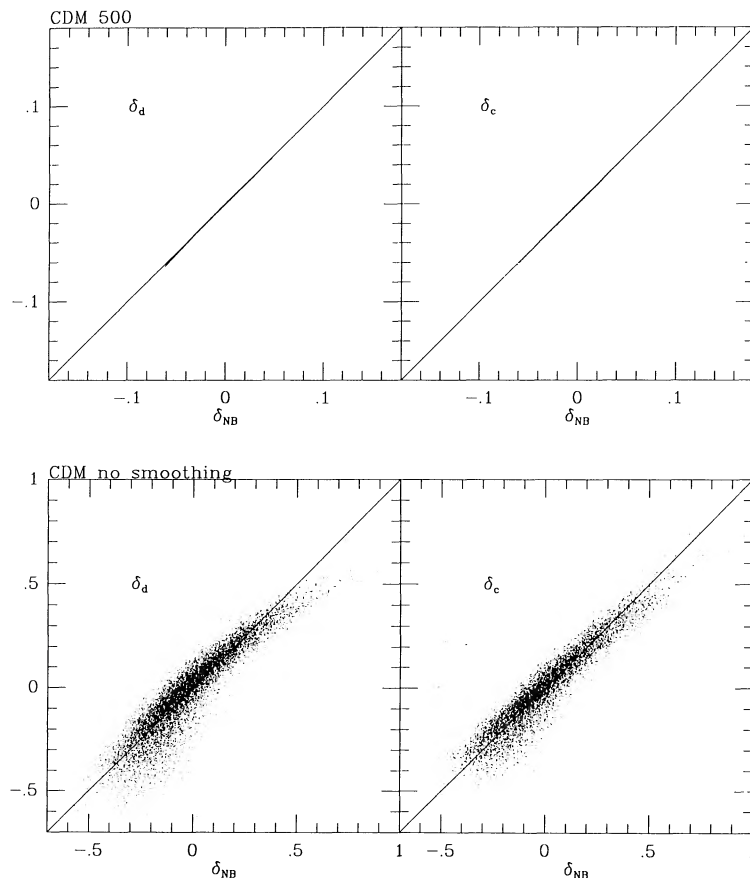


FIG. 5.—Densities in the Zel'dovich approximation vs. true densities in the initial time of the CDM  $N$ -body simulation. *Top*: Gaussian smoothed with 500  $\text{km s}^{-1}$ . *Bottom*: unsmoothed.

linear density fluctuations in the vicinity of a point. The nonlinear time dependence is not given by either of the linear modes and the time and position dependence do not separate as they do in the linear regime. Thus, nonlinear evolution may introduce a nonzero  $\text{div } v$  even at points where  $\delta = 0$  today.

Finally, the scatter near  $\delta = 0$  might reflect the error made when we assume zero pressure and zero vorticity.

The second question is how does the performance of the Zel'dovich approximation in the  $N$ -body simulations at points of large  $|\delta|$  compare to its performance in the spherical case, for example. They agree quite well for negative perturbations, but for large positive perturbations, while the order  $\delta_d < \delta_c$  is typically kept, both  $\delta_c$  and  $\delta_d$  tend to be smaller in the  $N$ -body case;  $\delta_d$  by about 10% and  $\delta_c$  by about 20% at  $\delta \simeq 3$ , for example. We can blame some of this effect on the CIC smoothing of the velocities discussed above (e.g., Fig. 5b). For example, if in some regions the velocity is anticorrelated with the density, this mass-weighted smoothing might result in a systematic underestimate of the velocity field, and therefore in its derivatives. This might be the case in the high density regions.

Another difference is the presence of collapsed regions in the  $N$ -body system, as in the real world, e.g., in galaxies or in the cores of clusters. In such regions orbits cross and the CIC velocity is an average over particles that may move in opposite streams. The result might therefore be smaller velocities and their partial derivatives relative to the velocity and derivatives in the spherical toy model where shell crossing was neglected. The Gaussian smoothing then carries the effect to large distances away from the collapsed cores, which results in a general reduction of the velocity gradients preferentially in regions of relatively high density. As long as the extent of the collapsed regions in the simulation is comparable to that in the real universe, and as long as the CIC smoothing scale is comparable to this scale, we believe one can regard the  $N$ -body simulations as a good nonlinear approximation for the real universe and use it as a reference for testing the densities in the Zel'dovich approximation and other quasi-linear approximations. Based on the different power spectra and smoothing lengths tried here, we conclude that the results are not very model-dependent. But more tests with different grid-cell sizes are required in order to quantify the exact sensitivity to the CIC smoothing in collapsed regions.

The bottom line is that the Zel'dovich approximations can provide a very useful estimate for the smoothed  $\delta(\mathbf{x})$  given the smoothed  $v(\mathbf{x})$ , all computed in Eulerian space. Based on the comparison with the smoothed  $N$ -body simulations we find that the rms error of the densities in the Zel'dovich approximation is less than 0.1 over the extended range  $-0.7 < \delta < 4.5$  for  $\delta_c$ , and over the more limited range  $-0.75 < \delta < 0.7$  for  $\delta_d$ . Thus,  $\delta_c$  is a very sensible approximation over the range of interest. A slightly more fancy approximation for  $\delta < 0$  is given by  $(\delta_c + \delta_d)/2$ , for which the rms deviation from the smoothed  $N$ -body results is less than 0.05.

In the original POTENT papers (e.g., Dekel et al. 1990) we calculated the density field using an elaborate iterative scheme based on the Lagrangian Zel'dovich displacements. This calculation was time-consuming, and it suffered from occasional convergence problems. The smoothed density was then computed using a very slow interpolation with a Gaussian point-spread function. We have now adopted  $\delta = \delta_c$  as our working scheme in the POTENT analysis. It gives similar results, but it is about 100 times faster, allowing the use of a finer spatial grid and many Monte Carlo noise simulations.

#### 4.2. Empirical Second- and Third-Order Corrections

The surprisingly small scatter of  $\delta_d$  about its mean, as seen for the  $N$ -body simulation in Figure 4, and the fact that its deviation from the true density is not too sensitive to the differences between the power spectra simulated or the smoothing lengths used, calls for an analytic fit to the scatter plot of  $\delta_d$ , which can serve as an empirical nonlinear correction. Guided by the fact that the continuity density in the Zel'dovich approximation is a good approximation over the whole quasi-linear regime, and that in almost all the special configurations studied in § 3.1 it can be expressed as a third-order polynomial of  $\delta_0$ , we find that the function

$$\delta = \delta_0 + 0.2\delta_0^2 + 0.05\delta_0^3 \quad (34)$$

is a good practical fit in the range  $-0.8 < \delta < 4.5$ , to an accuracy better than  $\pm 0.1$ , both for the CDM and neutrino simulations with either 500 or 1000  $\text{km s}^{-1}$  smoothing. As an illustration, this function is drawn in Figure 6 on top of the scatter plot corresponding to the CDM simulation with 500  $\text{km s}^{-1}$  smoothing. This empirical result could indeed be interpreted as an appropriately weighted average of the relations between  $\delta_c$  and  $\delta_0$  in the prototypical cases of generic symmetries in § 3.1; it is consistent with the structure being dominated by a mixture of filaments and pancakes. A similar approximation, to second order, can be derived analytically under the assumption that the local dimensionality of the flow remains constant (Nusser, Dekel, & Lynden-Bell 1991).

We also use the  $N$ -body simulations to test nonlinear corrections involving second derivatives of the sort  $\propto \nabla^2 v^2$ , as discussed in § 3.6. A good fit on the average is obtained for  $\delta = \delta_0 + 0.33\nabla^2 v^2$ , as shown in Figure 7 for the CDM simulation with 500  $\text{km s}^{-1}$  smoothing. (Note that this is just opposite to the "correction" obtained in eq. [22], demonstrating the fact that we could not have obtained a meaningful correction using a linear approximation for the time derivative.) But here, the rms scatter is much larger than in the Zel'dovich approximations, on the order of 0.3 over most of the quasi-linear range. This scatter, and the numerical disadvantages associated with the need to calculate second derivatives, make this empirical approach much less appealing than the continuity density of the Zel'dovich approximation (16), or the empirical approximation (34). Second-order corrections that include

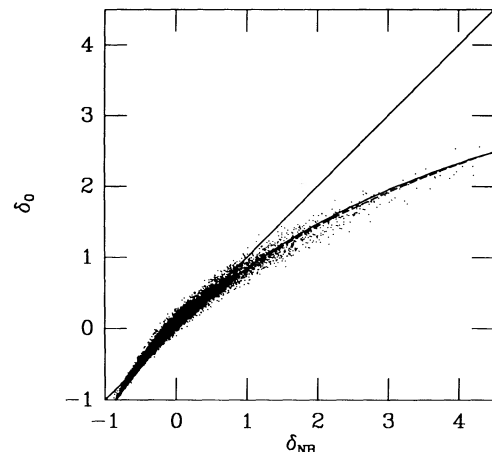


FIG. 6.—The empirical polynomial fit  $\delta = \delta_0 + 0.2\delta_0^2 + 0.05\delta_0^3$  (dashed) and its approximate inverse  $\delta_0 = \delta/(1 + 0.18\delta)$  (solid) on top of the scatter plot of the dynamical density of the Zel'dovich approximation  $\delta_d (= \delta_0)$  vs. the true density  $\delta$  from the CDM  $N$ -body simulation with 500  $\text{km s}^{-1}$  smoothing.

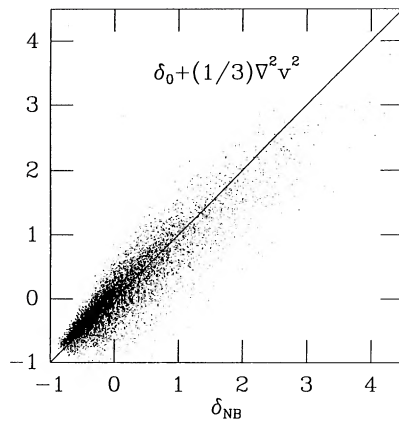


FIG. 7.—The empirical approximation  $\delta = \delta_0 + 0.33\nabla^2 v^2$  vs. true density in the  $N$ -body simulation; CDM with  $500 \text{ km s}^{-1}$  Gaussian smoothing.

pressure effects may do better, but they are more complicated to implement and, besides, why work hard when the simple  $\delta_c$  does so well?

#### 4.3. The Validity of the Approximations in an Open Universe

To test the validity of some of the approximations discussed above in an open Friedmann universe, we have applied them to a CDM simulation of an open model, in which the present density parameter is  $\Omega = 0.2$  and the amplitude of the fluctuations is normalized as before.

In the expressions for the densities in the Zel'dovich approximation, equations (16) and (19), we have substituted  $f(\Omega) = \Omega^{0.6}$ . Figure 8 is the  $\Omega = 0.2$  equivalent of Figure 4a. It shows  $\delta_d$  and  $\delta_c$  versus the true  $\delta_{\text{nb}}$  at  $10^4$  random grid points for two different smoothings:  $1000$  and  $500 \text{ km s}^{-1}$ . The behavior of the approximations is quite similar to the  $\Omega = 1$  case; both the systematic deviations and the scatter are of similar magnitude. A closer look reveals that  $|\delta_c|$  tends to be slightly larger than in the  $\Omega = 1$  case for large  $|\delta|$  values, which makes it a slightly better approximation at negative fluctuations and slightly worse at large positive fluctuations.

Also plotted in Figure 8 is the empirical third-order polynomial of equation (34), which has been determined by eyeball fit in the  $\Omega = 1$  case (Fig. 6). It turns out that with the simple  $\propto f(\Omega)^{-1}$  dependence of  $\delta_0$ , the same polynomial still provides a very good fit in the  $\Omega = 0.2$  case. Since, even with  $500 \text{ km s}^{-1}$  smoothing, the systematic deviation of the points from this fit is only on the order of the scatter, we conclude that the same polynomial can serve as a practical good approximation for  $\Omega = 0.2$  as well. This result will be found particularly useful in the inverse analysis discussed in the following section.

#### 5. VELOCITY FROM DENSITY

In some cases one wishes to reverse the process and recover the velocity field from a given density field. This is done, for example, in the iterative analysis of the *IRAS* galaxy redshift catalog, where the galaxies are assumed to trace the mass (Yahil et al. 1990).

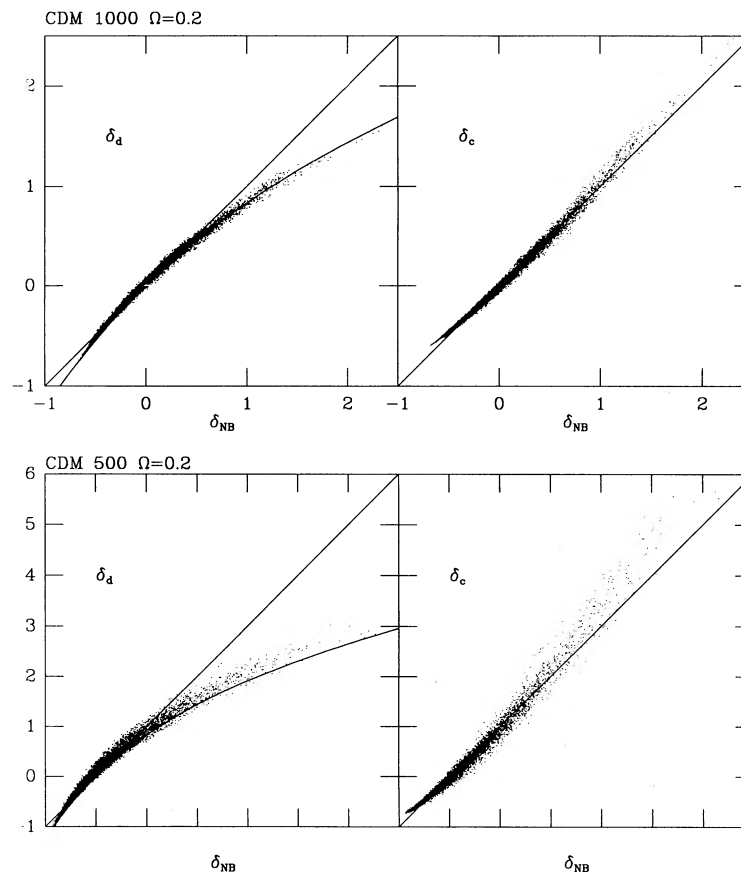


FIG. 8.—Densities in the Zel'dovich approximation vs. true densities in an open-model  $N$ -body simulation of CDM with  $\Omega = 0.2$  today. Also shown is the polynomial fit of Fig. 6.

In the linear regime the solution is simple (but not local). Given

$$\nabla \cdot \mathbf{v}(\mathbf{x}) = -Hf\delta_0(\mathbf{x}), \quad \mathbf{v} = -\nabla\phi_v, \quad (35)$$

the general solution is an integral over all space:

$$\phi_v(\mathbf{x}) = -\frac{Hf}{4\pi} \int \frac{\delta_0(\mathbf{x}')}{|\mathbf{x}' - \mathbf{x}|} d^3\mathbf{x}' + \phi', \quad \nabla^2\phi' = 0, \quad (36)$$

where  $\phi'$  vanishes for a perturbed Robertson-Walker universe. In practice, as long as the power spectrum drops steeply enough toward large scales, in particular if the power index of the density power spectrum is  $n \geq -1$ , the gradient of  $\phi_v$  is dominated by some finite neighborhood of  $\mathbf{x}$ . Based on the analysis of the  $N$ -body simulations (Fig. 4), we can tell that in the range  $|\delta| < 0.7$ , the linear approximation  $\delta_0$  typically approximates the real  $\delta$  with an accuracy of about 10%.

In the quasi-linear regime, the "linear" solution (36) is still valid for the dynamical density in the Zel'dovich approximation. However, we learned that for  $\delta \geq 1$  the continuity density of the Zel'dovich approximation is a much better approximation to the true density. Then, one could, in principle, solve for  $\mathbf{v}(\mathbf{x})$  and  $\phi(\mathbf{x})$  in the more complicated set of equations

$$\delta(\mathbf{x}) = \left\| I - (Hf)^{-1} \frac{\partial \mathbf{v}}{\partial \mathbf{x}} \right\| - 1, \quad \mathbf{v} = -\nabla\phi. \quad (37)$$

Unfortunately, we do not see an easy solution to this nonlinear set of elliptic differential equations and their boundary conditions.

A more practical approach is suggested as follows. We have noted in Figure 4, based on the smoothed  $N$ -body results, that the linear  $\delta_0$  (identical to the dynamical  $\delta_d$ ) and the true  $\delta$ , both associated with the same velocity field, show a relatively tight correlation. A simple approximate inverse of the polynomial fit (34) is

$$\delta_0 = \delta / (1 + 0.18\delta). \quad (38)$$

This is a good practical fit in the range  $-0.8 < \delta < 4.5$  (and beyond), to an accuracy better than  $\pm 0.1$ , for all the simulations and the various smoothing tested. This function is also shown in Figure 6.

The proposed procedure would be to first use the correlation (38) to translate the given true  $\delta$  to an equivalent  $\delta_0$  at all points, and then solve for  $\mathbf{v}(\mathbf{x})$  using  $\delta_0$  in the linear solution (36). This procedure will be tested in detail elsewhere.

## 6. SUMMARY AND CONCLUSIONS

Given the peculiar velocity field of a quasi-linear gravitating system,  $\mathbf{v}(\mathbf{x})$ , in comoving coordinates  $\mathbf{x}$ , alternative density fields can be computed locally under the assumption of Zel'dovich displacements, using the first partial derivatives of the velocity components in *Eulerian* space: the continuity density,

$$\delta_c = \left\| I - (Hf)^{-1} \frac{\partial \mathbf{v}}{\partial \mathbf{x}} \right\| - 1, \quad (39)$$

which ensures conservation of mass, and the dynamical density,

$$\delta_d = -(Hf)^{-1} \nabla \cdot \mathbf{v}, \quad (40)$$

which conserves momentum and actually coincides with the linear approximation,  $\delta_0$ .

Studying the difference between  $\delta_d$  and  $\delta_c$  in several generic configurations we find that both coincide and provide an exact solution in the case of a pure pancake, they differ at  $|\delta_0| \sim 1$  by about 25% in the most common case of a filament, and by 30%–40% in the spherical case. The worst difference is obtained in the case of an expanding filament, 100% already at  $\delta_0 = 0.62$ , but such a configuration is rare, and it reaches high densities only at a late time.

A comparison of the densities under the Zel'dovich approximation with the exact solution in the top-hat model yields that  $\delta_c$  and  $\delta_d$  carry errors of similar magnitudes and opposite signs such that  $\delta_d < \delta_{th} < \delta_c$ . The relative errors are about 14% at  $\delta = 1$ , 34%–53% at  $\delta = 4.5$ , and 13% at  $\delta = -0.5$ . The arithmetic average  $0.5(\delta_c + \delta_d)$  is a practical good approximation to the top-hat solution over the range  $-1 < \delta < 4.5$ .

The results for more generic configurations, as derived from  $N$ -body simulations of CDM and neutrino cosmologies with  $\Omega = 1$  and  $\Omega = 0.2$ , smoothed with a Gaussian of radius 500 or 1000 km s<sup>-1</sup>, are consistent with a certain mixture of the results for pancakes, filaments and spherical cases and are somewhat different from the top-hat results (mainly because the collapse is never really spherical, and mostly because of the smoothing over regions where shell-crossing occur). A useful (and elegant) working approximation is given by  $\delta_c$  over the range  $-0.7 < \delta < 4.5$ , with rms deviation from the  $N$ -body results of less than 0.1 everywhere. The average  $(\delta_c + \delta_d)/2$  has an rms deviation better than 0.05 for negative perturbations.

The exact second-order solution is much less useful because it is nonlocal. However, a third-order correction, motivated by the Zel'dovich approximation in the cases of special configurations, and by the "dimensionality" approximation (Nusser et al. 1991), has been determined empirically from the  $N$ -body simulations to be

$$\delta = \delta_0 + 0.2\delta_0^2 + 0.05\delta_0^3, \quad (41)$$

with an rms scatter better than 0.1 over the range  $-0.8 < \delta < 4.5$ . The same polynomial provides a good approximation for  $\Omega$  values in the range 0.1–1.

Attempts to apply linear time evolution in the dynamical equation which explicitly include a second-derivative term generally fail. The best correction proportional to  $\nabla^2 v^2$  has been determined empirically to be  $\delta = \delta_0 + 0.33\nabla^2 v^2$ , but with a large scatter on the order of 0.3 everywhere.

The continuity density derived from the Zel'dovich displacement field, or the empirical third-order polynomial given here, thus provide useful tools for reconstructing the mass density field from the quasi-linear velocity field. The three-dimensional velocity field itself can first be obtained from radial peculiar velocities using the potential flow analysis of Bertschinger & Dekel (1989). These approximations complete the POTENT analysis, allowing us to reconstruct all of the dynamical fields from the observed radial peculiar velocities of galaxies all the way to the total (dark plus luminous) mass density distribution.

The mass density fluctuations can be compared directly with the predictions of competing theoretical scenarios, independently of questions about biasing. These tests should constrain models of the fluctuation generation in the early universe and may clarify the nature of the dark matter. Even more importantly, a comparison of the distribution of mass with that of luminous galaxies on large scales can constrain the poorly understood process of galaxy formation.

The inverse problem of extracting the velocity field from a

given density field involves non-local integrals even in the linear approximation. The relatively tight correlation seen in the different  $N$ -body simulations between the true and the dynamic (= linear) densities that are derived from the true velocities under the Zel'dovich approximation, with an rms width of less than 0.1, suggests the following practical quasi-linear scheme. Use an empirical fit based on the  $N$ -body simulations to translate the given density to an equivalent dynamical density and then solve for the velocity using the linear procedure. A useful empirical fit of this sort, good to an accuracy of about 0.1 in the range  $-0.8 < \delta < 4.5$  for  $0.1 \leq \Omega \leq 1$ , is given by

$$-\nabla \cdot \mathbf{v} = \delta / (1 + 0.18\delta). \quad (42)$$

This method will be tested carefully in another paper.

#### REFERENCES

- Bertschinger, E., & Dekel, A. 1989, *ApJ*, 336, L5  
 Bertschinger, E., Dekel, A., Faber, S. M., Dressler, A., & Burstein, D. 1990, *ApJ*, 364, 370  
 Bond, J. R., & Szalay, A. 1983, *ApJ*, 274, 443  
 Davis, M., Efstathiou, G., Frenk, C., & White, S. D. M. 1985, *ApJ*, 292, 371  
 Dekel, A., Bertschinger, E., & Faber, S. M. 1990, *ApJ*, 364, 349  
 Dekel, A., & Rees, M. J. 1987, *Nature*, 326, 455  
 Dressler, A., Lynden-Bell, D., Burstein, D., Davies, R. L., Faber, S. M., Terlevich, R. J., & Wegner, G. 1987, *ApJ*, 313, 42  
 Lightman, A., & Schechter, P. 1990, preprint  
 Lynden-Bell, D., Faber, S. M., Burstein, D., Davies, R. L., Dressler, A., Terlevich, R. J., & Wegner, G. 1988, *ApJ*, 326, 19  
 Nusser, A., Dekel, A., & Lynden-Bell, D. 1991, in preparation  
 Peebles, P. J. E. 1980, *The Large-Scale Structure of the Universe* (Princeton: Princeton Univ. Press)  
 Pierce, M. J., & Tully, R. B. 1988, *ApJ*, 330, 579  
 Shandarin, S. F., Doroshkevich, A. G., & Zel'dovich, Ya. B. 1983, *Soviet Phys.—Uspekhi*, 26, 1  
 Strauss, M. A., Davis, M., Yahil, A., & Huchra, J. P. 1990, preprint  
 Yahil, A., Strauss, M. A., Davis, M., & Huchra, J. P. 1990, preprint  
 Zel'dovich, Ya. B. 1970, *A&A*, 5, 20